Geotechnical Engineering Journal of the SEAGS & AGSSEA Vol. 49 No. 4 December 2018 ISSN 0046-5828

Fatigue Performance of Geosynthetic Reinforced Two-Layered Asphalt Concrete Beams

V. Vinay Kumar[1] and S. Sireesh[2*]

[1]*Doctoral student, Department of Civil Engineering, Indian Institute of Technology Hyderabad, Kandi, Sangareddy, India*

[2]*Associate Professor, Department of Civil Engineering, Indian Institute of Technology Hyderabad, Kandi, Sangareddy, India*

**Corresponding author, E-mail*: sireesh@iith.ac.in

ABSTRACT: One of the most common rehabilitation techniques adopted for distressed pavements is hot mix asphalt (HMA) overlay. It is often practiced to include geosynthetic interlayers before placing an HMA overlay. The interlayers in HMA overlay not only improves the performance life of the pavement structure by increasing the stiffness, but also, reduces the maintenance cost and the cost of construction by reducing the thickness of HMA overlay.

In the current study, the performance of geosynthetic reinforced two layered asphalt beams is evaluated in two stages. During the first stage, the fatigue performance of the two layered asphalt beams is evaluated using a flexural fatigue test (four point bending). During the second stage, the fracture energy required for crack propagation in the beams during fatigue loading and the corresponding tensile stiffness of two layered asphalt beams with and without geosynthetic interlayers are determined using Fenix test. Three types of geosynthetics, namely biaxial polyester grids, woven geo-jute mat and biaxial polypropylene grids are used in the study. The results from fatigue and Fenix tests indicated that the fatigue life and the tensile stiffness of the geosynthetic reinforced asphalt beams have drastically increased against the control specimens. A 30 times increase in fatigue life is noticed in polyester grid reinforced asphalt beams against unreinforced beams at 10 mm vertical deformation, which is attributed to the increase in tensile stiffness of the specimens from 7.3 kN/mm to 17.6 kN/mm. A linear regression equation is proposed to correlate the normalized complex modulus and tensile stiffness index to estimate the complex modulus of the geosynthetic reinforced asphalt beams.

KEYWORDS: Fenix test, Flexural fatigue test, Geosynthetics, HMA overlay

1. INTRODUCTION AND BACKGROUND

The performance of existing flexible pavements is often observed to be affected by various detrimental factors like heavy traffic loads, aging of pavement system, environmental factors etc. These factors further accelerate the need for rehabilitation or maintenance of the existing pavement system to provide a safe and efficient ride quality to the road users (Virgili et al. 2009). The rehabilitation technique traditionally consists of laying an asphalt overlay of an appropriate thickness. Further, to improve the mechanical properties of the asphalt overlays, geosynthetic reinforcements are provided between the pavement layers (Ferrotti et al. 2012; Kumar et al. 2017). The introduction of geosynthetic interlayers not only improves the mechanical properties, but also considerably reduces the thickness of asphalt overlays and thereby the construction cost. Besides, the introduction of geosynthetics in the pavements at different levels often results in various types of advantages. In the case of unpaved roads, geosynthetics are placed above the subgrade to provide functions like reinforcement, separation, filtration and drainage in the pavement system (Gurung, 2003). Whereas, in the case of paved roads, the location of geosynthetics above the subgrade results in the reduction of rutting and permanent deformations (Brown et al. 1985; Komatsu et al. 1998). Similarly, when placed at the interface of base course and surface layers, they improve the performance by extending the fatigue life and a reduction in surface layer thickness (Brown et al. 1985, Virgili et al. 2009). Besides, the geosynthetics, when placed at the interface of existing pavement layer and new asphalt overlay, reduces the effect of reflective cracking in HMA overlays (Caltabiano and Brunton, 1991; Austin and Gilchrist, 1996; Elseifi and Al-Qadi, 2003; Kumar and Saride, 2017; Saride and Kumar, 2017). The elimination of reflective cracking helps to improve the fatigue performance of HMA overlays as the reflective cracking is the primary mode of failure often witnessed in HMA overlays.

Researchers worldwide have developed various laboratory and field techniques to evaluate the effectiveness of geosynthetics in improving the fatigue performance of asphalt overlays (Khodaii et al. 2009). The inclusion of geogrid interlayers in the pavement system reduced the permanent deformations and improved the traffic benefit ratios (TBR) (Chen et al. 2009) when the geogrid interlayer was introduced at the interface of base and subgrade. The fatigue life of geogrid reinforced asphalt overlays in the field were observed to be increased by about 80% when the geogrid is placed at the bottom of overlay against no interlayer case (Guo and Zhang, 1993). Similarly, an improvement in the performance of fiber grid reinforced specimens was achieved, when the grid is placed at the bottom of asphalt layer (Bocci et al. 2007).

Brown et al. (2001) performed four point bending tests on grid reinforced and unreinforced specimens and found that the improvement in performance of grid reinforced specimens were basically due to the increase in stiffness of the reinforced specimens. However, Austin and Gilchrist (1996) and Kumar and Saride (2017) showed from their experimental study that the presence of reinforcement does not increase the stiffness of the specimen tested, in addition, the reinforcement does not also allow the stiffness of the specimens to reduce quickly. Shukla and Yin (2004) and Pasquini et al. (2012) reported that the mechanical properties of the pavement system were improved with the introduction of geosynthetic reinforcements. Similarly, Mahrez et al. (2005) observed that the fiberglass grid reinforcement provided in the asphalt pavement layers improved the tensile strength of asphalt pavement system by increasing its capacity to absorb the energy dissipated during repeated loading conditions.

Further, the energy dissipated during the cracking process of gyratory compacted asphalt mixtures were determined using a direct tensile strength test known as Fenix test (Miro et al. 2014). Perez-Jimenez et al. (2012) used Fenix test to provide an approach to the fatigue performance of different asphalt mixtures by correlating the fatigue test and Fenix test results.

From the literature, it can be summarized that the inclusion of geosynthetics in new asphalt pavements has shown a considerable amount of performance improvement. However, these studies mostly addressed the performance improvement of new asphalt pavement layers. The actual field scenario would be entirely different when an asphalt overlay is being placed over an old distressed pavement with a geosynthetic reinforcement at the interface. The existing results from the literature in terms of energy dissipation and fatigue life cannot be extrapolated to the asphalt overlays. Hence, in the current study, an attempt has been made to replicate the field scenario in a laboratory scale by performing repeated fatigue (four point bending) tests on two layered specimens with old pavement as the bottom layer and an HMA overlay with and without geosynthetic reinforcement placed at the interface. The energy dissipated during the cracking process and the tensile stiffness of the two layered specimens are determined using Fenix test.

2. MATERIALS

2.1 Asphalt concrete and binder tack coat

The asphalt concrete (AC) mix used in the overlay was prepared at the mix plant and transported to the laboratory. The mix has a nominal aggregate size of 13 mm and consists of penetration grade 60/70 bitumen as a binder with an optimum binder content of 5.5 %. The AC mix has a strength (Marshall stability) of 14.25 kN and a flow value of 2.5 mm. The binder tack coat used in the current study is penetration grade 60/70 bitumen, having a penetration value of 66 and the properties of the binder are listed in Table 1.

Table 1 Properties of binder tack coat

Sl No.	Properties	Values
1	Penetration (1/10th mm)	66
2	Ductility (cm)	100+
3	Specific gravity	1.01
4	Viscosity, Brookfield at 60 ^{0}C (centipoise)	460
5	Softening point (^{0}C)	52
6	Flash point (^{0}C)	340
7	Fire point (^{0}C)	365

2.2 Geosynthetic reinforcements

In the current research program, three different types of reinforcing materials were used to study the flexural fatigue performance of the geosynthetic reinforced asphalt beams against the control specimen. The reinforcing materials were selected based on their material composition, aperture size and tensile properties. The materials used in the current study are:

Geo-jute mat (R1): Mat is produced either by machine or hand weaving of natural geo-jute materials like threads and/or fibers. The geo-jute mat (Figure 1) has ultimate tensile strength of 25 kN/m (machine direction-MD) and 20 kN/m (cross machine direction-CMD) at a strain of 5 % and 12 % respectively.

Figure 1 Woven Geo-jute mat (R1)

Bi-axial polypropylene grid (R2): The bi-axial grid is produced using a polypropylene material, has a tensile strength of 30 kN/m (MD and CMD) at a strain of 10-12 % and an aperture of 40×40 mm^2 area. Figure 2 shows a bi-axial polypropylene grid used in the current study.

Polyester grid (R3): The grid is manufactured using a high tenacity and high molecular weight polyester yarns, which are knitted together to form a grid structure as shown in Figure 3. The grid has an aperture opening of 18×18 mm^2 area and has a tensile strength of 40 kN/m (MD and CMD) at a strain value of 18-20 %. The grid is also coated with a polymer modified binder to improve the bonding between the adjacent layers.

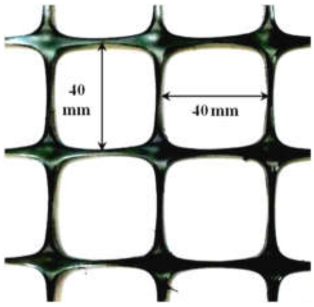

Figure 2 Biaxial polypropylene grid (R2)

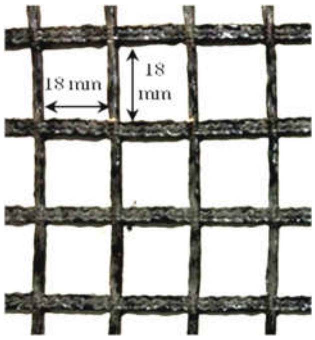

Figure 3 Polyester grid coated with polymer modified bitumen (R3)

2.3 Two layered asphalt specimen preparation

The geosynthetic reinforced two layered asphalt specimens for flexural fatigue test and Fenix test were prepared in different stages. During the first stage, the geosynthetic reinforced two layered asphalt slab of 400 mm length, 300 mm width and 90 mm thickness was prepared in the laboratory as shown in Figure 4.

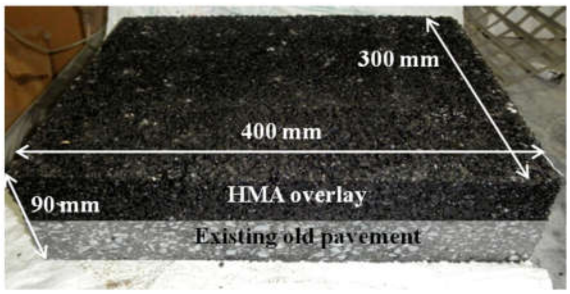

Figure 4 Two layered asphalt slab prepared in the laboratory

The two layered asphalt slab consists of an old deteriorated pavement slab of 45mm thickness as the bottom layer, a binder tack coat applied at the rate of 0.25 kg/sq.m, geosynthetic reinforcement and an HMA overlay. The old deteriorated pavement slab was carefully extruded from the existing highway during the rehabilitation program and further cut into the required dimensions. The air void content (7%) in the HMA overlay was maintained constant to maintain homogeneity in the specimens prepared. During the next stage, the beam specimens for both flexural fatigue and Fenix tests were prepared by cutting the two layered asphalt slab as per the experimental requirements. The two layered asphalt slab was cut into asphalt beams of 50 mm width, 400 mm length and 90 mm thickness for flexural fatigue test. Similarly, for Fenix test, the slab was cut into a rectangular specimen of 100 mm length, 50 mm width and 65 mm (45 mm overlay + 20 mm old layer) thickness. The detailed procedure of two-layered asphalt specimen preparation is explained by Kumar and Saride (2017) and Saride and Kumar (2017).

3. EXPERIMENTAL PROGRAM

The experimental program consists of applying repeated load on the two layered asphalt beam specimens under four point loading conditions and applying a tensile load on the two layered specimens using Fenix test to evaluate the performance of geosynthetic reinforced asphalt beams against the control specimen.

3.1 Flexural fatigue test

A conventional four point bending test setup as shown in Figure 5 was used to apply the repeated load on the asphalt beams under stress controlled mode as per ASTM D7460. The loads were applied repeatedly until the specimens failed completely and the corresponding vertical deformations were measured at the mid-span using the actuator displacement sensors. The load was applied using a computer controlled servo hydraulic actuator system at a frequency of 1 Hz with a haversine loading pattern. The loading pattern was selected in such a way that it replicates the live traffic movement (equivalent to a single axle load contact pressure of 550 kPa) on the specimens tested. The maximum load to be applied to replicate a contact pressure of 550 kPa was determined using equation 1. A maximum load of 0.6 kN and a minimum load of 0.06 kN (10% of peak load) was applied as a seating load. The seating load was applied to avoid rocking action of the specimens tested, as explained by Murdock and Kesler (1958) and Paul et al. (2015). The mid-span vertical displacements measured using displacement sensors at various load cycles can be used to calculate the corresponding maximum flexural strains using equation 2 (ASTM D 7460).

$$\sigma_f = \frac{Pl}{bh^2} \quad (1)$$

$$\epsilon = \frac{108\delta.h}{23l^2} \quad (2)$$

Where, σ_f is the maximum stress in MPa, P is the maximum load applied in kN, l is the length of the beam in m, b is the width of the beam in m, h is the thickness of the beam in m, ϵ is the maximum strain in the specimen, and δ is the vertical deformation at mid-span of the specimen in mm.

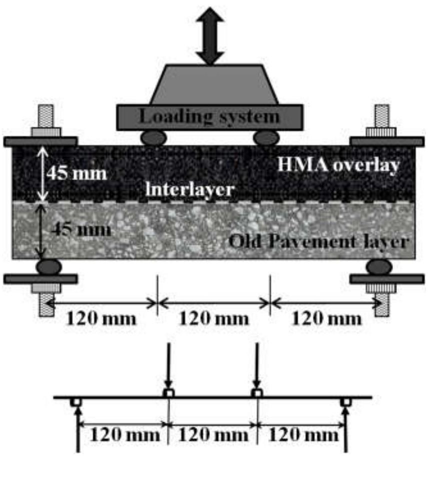

Figure 5 Schematic of flexural fatigue test setup

A typical applied flexural stress versus the calculated maximum flexural strain curve for the control or no reinforcement (NR) specimen is plotted as shown in Figure 6. It can be cross verified from Figure 6, that a maximum flexural stress of 550 kPa and a minimum (seating) flexural stress of 55 kPa is applied repeatedly to replicate the live traffic condition. It is also observed that there is a decrease in the flexural strain with the increase in the number of load repetitions. The high strains observed initially are due to the initial high vertical deformations recorded at the mid-span. The flexural stress-strain pattern is not constant and varies with the type of reinforcement placed in the specimens tested.

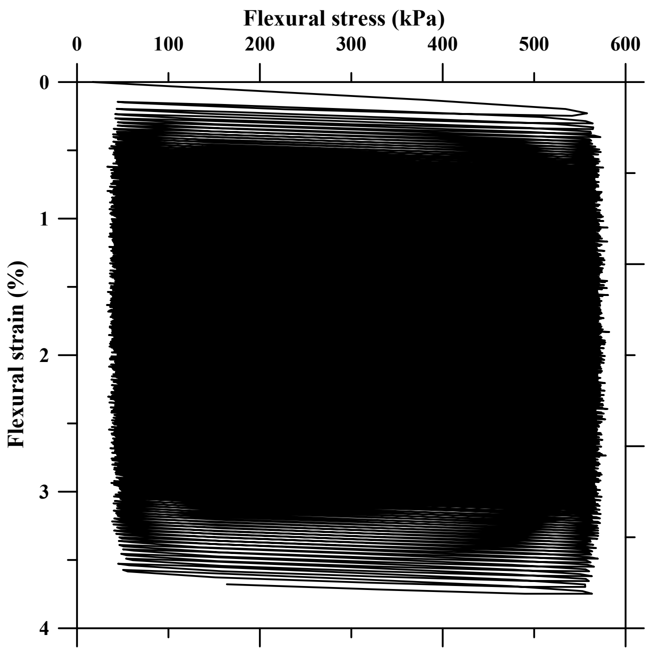

Figure 6 Typical flexural stress-strain plot for control (NR) specimen

3.2 Fenix test

The Fenix test is a direct tensile strength test performed on one-half of a cylindrical specimen prepared by gyratory or Marshall compaction. In the current study, the cylindrical specimen has been replaced with a rectangular two layered asphalt specimen as shown in Figure 7.

A 6 mm deep notch is made in the bottom portion of the rectangular specimen and is glued with an epoxy to the steel plates placed 6 mm apart. The notch represents the pre-crack in the old pavement and also guides the initiation of crack in the specimen during the testing process. The specimen-plate assembly is then placed in a tensile testing machine and a constant vertical displacement at a rate of 1 mm/min is applied until the specimen cracks completely. Figure 7 shows the schematic of Fenix test setup and a typical load-displacement curve with typical quantities required for the analysis.

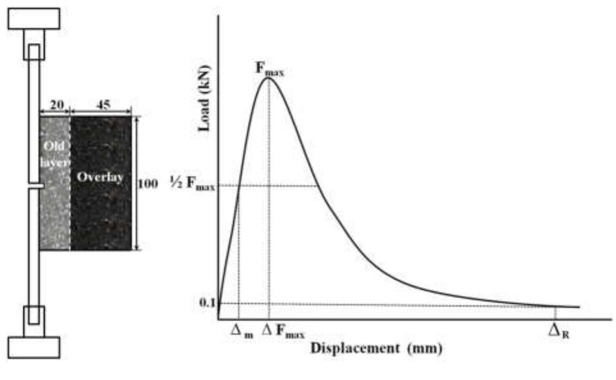

Figure 7 Schematic of Fenix test setup and typical output curve

The load applied and the corresponding displacements are continuously recorded until the specimen fails (cracks) completely. The energy dissipated during the process is calculated using equations 3 and 4.

$$G_D = \frac{W_D}{h.l} \tag{3}$$

Where, G_D is the energy dissipated during testing process in J/m^2, W_D is the work done during the test, the area under the load-displacement curve in kN-mm, h is the specimen thickness in m and l is the length of the specimen in m.

$$W_D = \int_0^{\Delta_R} F.du \tag{4}$$

Where, F is force in kN, u is displacement in mm and Δ_R is the displacement at F=0.1 kN, post-peak load curve in mm. The tensile stiffness index is obtained from equation 5.

$$I_{RT} = \frac{1/2.F_{\max}}{\Delta_m} \tag{5}$$

Where, I_{RT} is tensile stiffness index in kN/mm, F_{max} is maximum load in kN and Δ_m is the displacement at ½ $F_{\max}$ in mm.

4. RESULTS AND DISCUSSIONS

4.1 Fatigue test results

The dynamic four-point load test performed on the two layered asphalt specimens under stress controlled mode helps to evaluate the overall performance of geosynthetic reinforced asphalt beams against the unreinforced asphalt beams. The repeated load was applied on each specimen until its failure. For every load cycle applied on the specimen, an increase in the vertical deformation was observed. The cumulative increase in the vertical deformation further leads to a complete fracture of the specimen. The results of the flexural fatigue tests are presented in Table 2 and it can be clearly seen that initially at a vertical deflection of 1 mm, the performance of all the specimens are similar with same number of load repetitions. However, as the vertical deformation increases there is a clear difference in resisting the number of load repetitions by unreinforced and the geosynthetic reinforced specimens. The fatigue life (no. of load repetitions, N) of the unreinforced asphalt beams is observed to be about 325 cycles at a vertical deformation of 10 mm and found very little increase, thereafter at 20 mm deformation, representing a failure.

Table 2 Summary of flexural fatigue test results

Specimen	Number of load cycles, N			
	VD=1mm	VD=5mm	VD=10mm	VD=20mm
NR	7	151	325	366
R1	7	226	503	823
R2	7	265	1730	7990
R3	7	1199	8639	19053

*VD-vertical deformation

However, the geosynthetic reinforced asphalt beams have shown up to a 7 fold improvement in fatigue life when the vertical deformation increased from 5 mm to 10 mm. The fatigue life of the reinforced beams continues to increase even up to 20 mm, before the sign of failure. This is due to the reinforcement effect of the geosynthetics provided at the interface. The failure pattern of the unreinforced and the geosynthetic reinforced asphalt beams (R1, R2 and R3) are shown in Figure 8. These pictures are captured from a high resolution camera used in digital image correlation technique.

It can be seen that the crack has initiated from bottom face of the beam and propagates through the old pavement and reflects on the asphalt
overlay (top layer). The influence of the geosynthetic reinforcement can be visualized from Figure 8, where the performance of R3 specimen is high in resisting the crack propagation against R1 and R2 specimens, respectively.

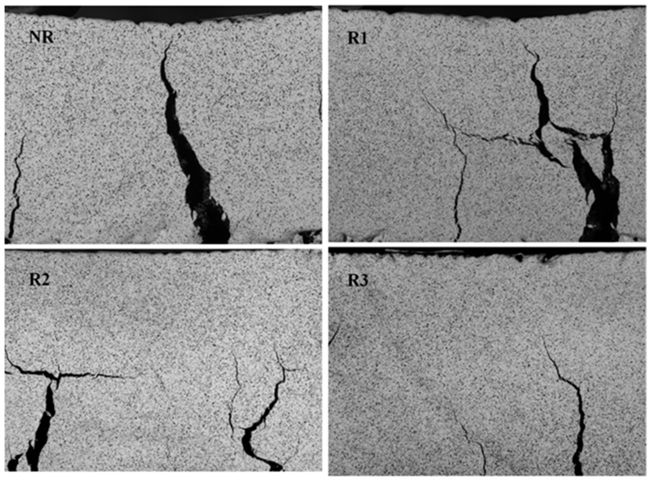

Figure 8 Failure patterns of different two layered asphalt beams

Initially, at a very low vertical deformation (about 1 mm), the effect of reinforcement is negligible or nil. When the vertical deformation has increased to 5 mm, the influence of reinforcement is witnessed. The geosynthetic reinforcement intervenes the vertical crack and absorbs the crack energy (tensile) and dissipates it in lateral direction at the interface, hence the improvement in the fatigue life. The amount of energy absorbed, which is equivalent to the energy dissipated in terms of number of load cycles, is entirely dependent on the type of reinforcement and the bonding characteristics between the reinforcement and the asphalt layers. Hence, it is very important to choose an appropriate tack coat which can effectively bind the reinforcement and the asphalt layers. This fact helps us to understand the importance of reinforcement in improving the performance (fatigue) life of the asphalt overlays. Among different reinforcements used in the study, R3 specimens have shown the highest performance by withstanding a maximum number of load repetitions of about 19000 cycles at a vertical deformation of 20 mm. In addition, the effectiveness of the reinforcement also depends on the failure tensile strain at the peak tensile stress of the material. The R3 sample has a peak tensile stress of 40 kN/m at a tensile strain of 20%, which is in line with the failure strain observed in the reinforced asphalt beams, lead to a high fatigue life in these specimens.

Further, the performance improvement in fatigue life of the reinforced specimens can be quantified using a non-dimensional factor, fatigue performance improvement factor (I_{Nf}) which is very similar to the traffic benefit ratio (TBR) used in estimating the performance of pavement systems. The performance improvement factor can be defined as the ratio of performance life of reinforced specimens to the performance life of unreinforced specimen at a given vertical deformation and mathematically expressed as:

$$I_{Nf} = \frac{N_R}{N_{NR}} \tag{6}$$

Where, I_{Nf} is the fatigue performance improvement factor, N_R is the fatigue life of geosynthetic reinforced specimens and N_{NR} is the fatigue life of unreinforced specimen in-terms of number of load cycles at a given vertical deformation.

Figure 9 presents the variation of I_{Nf} with vertical deformation. It can be clearly distinguished that there is a clear improvement in the performance life of the reinforced specimens. The R1 specimen showed the least improvement with a I_{Nf} of only 2.75, whereas, the R3 specimen with a I_{Nf} of 52.5 performed better than the rest tested showing a highest improvement in fatigue life. On the other hand, the R2 specimen with a I_{Nf} of 22.5 could only display an intermediate performance. From Figure 9, it can also be understood that the I_{Nf} for R2 and R3 specimens increases remarkably after reaching a vertical deformation of 5 mm until 20 mm. The main reason for this improved performance is due to an increase in the stiffness of specimens due to the introduction of reinforcement.

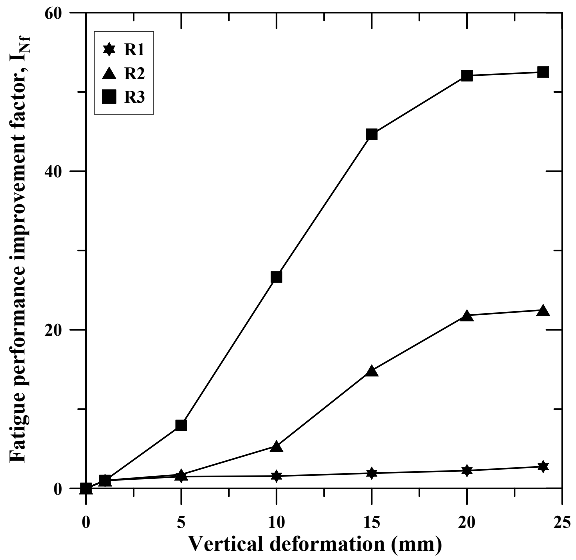

Figure 9 Variation of I_{Nf} with vertical deformation

The stiffness with respect to the number of load cycles is shown in Figure 10. It can be observed that the stiffness of R1 specimen is much higher than the rest. The increase in the stiffness can also be presented in terms of normalized complex moduli for the asphalt specimens, which can be calculated using equation 7 (ASTM D-7460).

$$NCM = \frac{S_i \times N_i}{S_o \times N_o} \tag{7}$$

Where, NCM is the normalized complex modulus, S_i is the stiffness of asphalt beam at i^{th} cycle, N_i is i^{th} cycle and S_o is the initial stiffness of asphalt beam, N_o is cycle corresponding to initial stiffness.

The normalized complex modulus is presented with number of load cycles in Figure 11. It can be clearly observed from Figure 11 that the complex moduli of the geosynthetic reinforced two layered asphalt specimens are higher than the control specimen with R3 specimen having a higher normalized complex modulus of 343. The high complex modulus for R3 specimen is due to the high tensile stiffness of the polyester material. The geosynthetic reinforcements of different material composition and mechanical properties as explained in s ection 3.2 have proven to improve the performance of asphalt overlays. However, the amount of improvement varies due to the material properties like the material composition, aperture size, thickness and tensile strength.

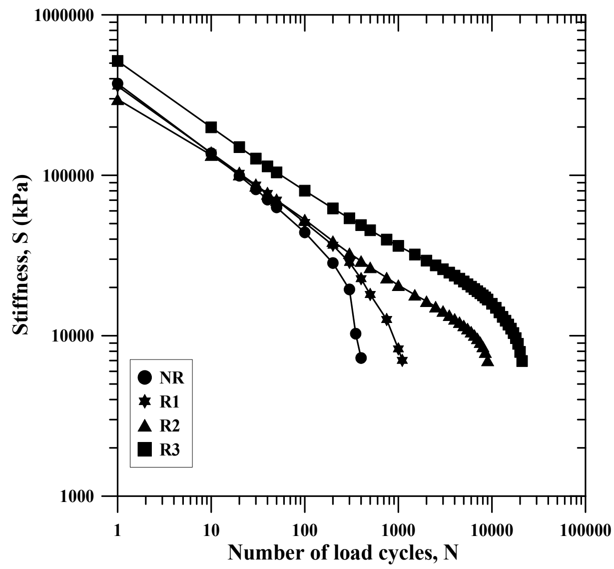

Figure 10 Variation of stiffness with number of load cycles

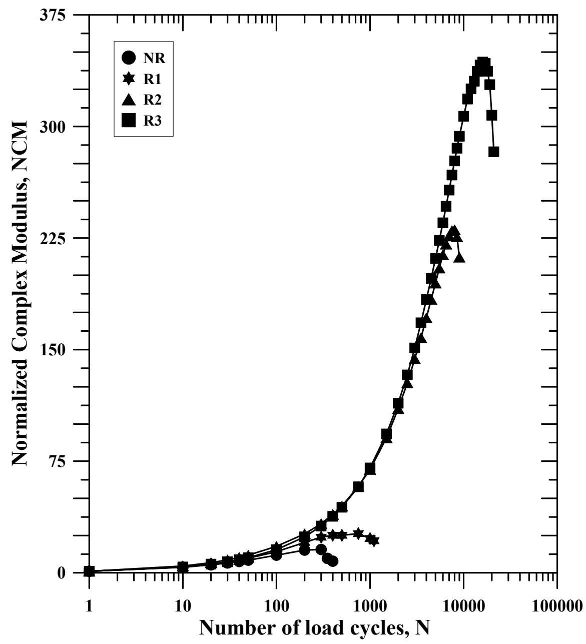

Figure 11 Variation of normalized complex modulus with number of load cycles

4.2 Fenix test results

The Fenix test performed on the two layered rectangular asphalt specimens helps to understand the cracking behavior of reinforced and unreinforced asphalt specimens based on the energy dissipated. The dissipated energy can be calculated from equation 3.

The summary of Fenix test results has been presented in Table 3 and it is seen that the energy dissipated during the cracking process is high in the case of reinforced specimens compared to the control specimen. This fact suggests that the reinforcement placed at the interface of old and new pavement layers helps to improve the cracking resistance potential of asphalt overlay by improving the tensile stiffness of the reinforced specimens.

Table 3 Summary of Fenix test results

Specimen	Peak load, F_{max} (kN)	Displacement at peak load, Δ_{max} (mm)	Displacement at F=0.1 kN, ΔR (mm)	Dissipated energy, GD (J/m2)	Tensile stiffness index, I_{RT} (kN/mm)
NR	0.43	0.27	4.3	305	7.3
R1	0.50	0.37	4.0	340	10.7
R2	0.60	0.37	6.0	610	13.4
R3	0.73	0.37	6.5	786	17.6

The tensile stiffness index of each specimen is calculated using the equation 5 and tabulated in Table 3. Among the reinforced specimens, the dissipated energy in R3 specimen at a tensile stiffness index of 17.6 kN/mm is highest, about 786 J/m^2, while the energy dissipated in R2 and R3 specimens are 610 J/m^2 and 340 J/m^2, respectively at a tensile stiffness indices of 13.4 kN/mm and 10.7 kN/mm. It can be observed from Figure 11 and Table 3 that the tensile stiffness index is higher for the specimens with higher complex modulus values (reinforced specimens). Hence, the presence of reinforcement at the interface of old and new pavement layers improve the modulus and stiffness of the specimens and hence, a greater resistance to fracture or cracking.

4.3 Correlation between fatigue and Fenix test results

The results obtained from the fatigue and Fenix tests suggest that the moduli of the specimens are related to their stiffness. In this regard, an attempt has been made to correlate the modulus parameter obtained from the fatigue tests and the corresponding tensile stiffness index obtained from the Fenix tests. The variation of normalized complex modulus with tensile stiffness index for all the specimens tested is presented in Figure 12. It can be observed that the modulus increases with an increase in the tensile stiffness index of the specimens. The results are observed to correlate well with a coefficient of regression (R^2) equal to 0.92.

Although, the correlation coefficient is obtained from three points (test results) in the current study, the correlation coefficient could be further improved by performing more number of tests on various grades of bituminous concrete, geosynthetic-interlayers and different temperatures.

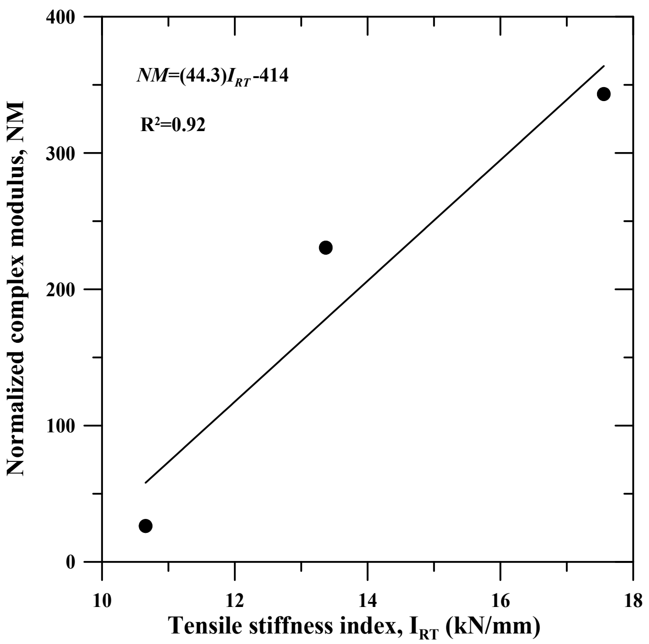

Figure 12 Variation of normalized complex modulus (NM) and tensile stiffness index (I_{RT})

A similar correlation between fatigue (3-point bending) and Fenix test parameters were proposed by Perez-Jimenez et al. (2012) for different types of bituminous mixtures as shown in equation 8.

$$MD = 1722.2 I_{RT} - 4271 \quad (8)$$

Where, MD is the dynamic modulus in kPa, I_{RT} is the tensile stiffness index in kN/mm.

Based on the equation 8, the predicted dynamic modulus of the NR sample from the current study is found to be 8351 kPa, however, the actual measured modulus from the fatigue test is about 63084 kPa, which is about 7.5 times the predicted value. In addition, for the reinforced beams (R3), the predicted dynamic modulus is about 25,965 kPa against the measured value of 104270 kPa. The great difference between the measured and predicted values from equation 8 may be attributed to the condition of the asphalt beams. In their study, Perez-Jimenez et al. (2012) have prepared single layered asphalt beams of different grades and tested at different temperatures to develop the correlation. Hence, the equation 8 is mostly applicable for unreinforced single asphalt layers. This implies that there is a need for the development of similar correlation between the complex modulus and the stiffness index for two layered geosynthetic reinforced asphalt concrete beams.

The accuracy of the proposed correlation can be improved by performing number of such tests with different geosynthetic interlayers and grades of asphalt concrete.

5. CONCLUSIONS

In the current study, the performance of geosynthetic reinforced asphalt concrete beams were evaluated using flexural fatigue and Fenix tests and the following conclusions are drawn:

The fatigue life of geosynthetic reinforced asphalt beams is observed to improve drastically against the unreinforced specimens. However, the asphalt beams reinforced with geo-jute mat has shown only a moderate improvement in the fatigue life (I_{Nf} of 2.75), whereas, the asphalt beams reinforced with polyester grid and polypropylene grids have shown high fatigue life, I_{Nf} of 52.5 and 22.5 respectively at 20 mm deformation. This is attributed to the tensile strength of individual geosynthetic material and an increase in the modulus of the reinforced asphalt beams. The increase in the modulus was achieved due to an increase in the tensile stiffness of the specimens or rather a very slow reduction in the modulus.

In addition, to understand the influence of geosynthetic reinforcement in the overall performance improvement, Fenix tests were conducted to determine the energy dissipated during the crack propagation and tensile stiffness of the specimens. It was inferred that the amount of energy dissipated (or required) to propagate the cracks developed during the fatigue tests in the case of geosynthetic interlayered asphalt beams is very high due to the improved tensile stiffness. The specimen reinforced with polyester grid (R3) has shown a greater resistance to cracking with an energy as high as 785 J/m^2 and a tensile stiffness index of 17.6 kN/mm. It is also observed that the resistance offered by the geosynthetic reinforcement depends on the peak tensile strength and tensile strain, aperture opening and the bonding properties of the geosynthetic material.

A reasonably good correlation was obtained between the normalized complex moduli (fatigue test) and the tensile stiffness (Fenix test) of the two layered asphalt beams with geosynthetic interlayers with a coefficient of regression (R^2) equal to 0.92. It was noticed that the normalized complex moduli of the asphalt layer is directly proportional to the tensile stiffness of the beam. The correlation coefficient can be improved further by performing more number of tests on various grades of bituminous concrete and geosynthetic interlayers. The correlation is highly useful in predicting the complex modulus of a geosynthetic reinforced asphalt layer with known tensile stiffness index, as performing Fenix test is much easier at a laboratory scale.

6. REFERENCES

ASTM D7460. "Standard Test Method for Determining Fatigue Failure of Compacted Asphalt Concrete Subjected to Repeated Flexural Bending".

Austin, R. A., and Gilchrist, A. J. T. (1996) "Enhanced performance of asphalt pavements using geocomposites". Geotextiles and Geomembranes, 14, pp. 175-186.

Bocci, M., Grilli, A., Santagata, F. A., and Virgili, A. (2007) "Influence of Reinforcement Geosynthetics on Flexion Behaviour of Double-layer Bituminous Systems", In: Proceedings of International Conference: Advanced Characterisation of Pavement and Soil Engineering Materials, Athens.

Brown, S. F., Brunton, J. M., Hunghes, D. A. B., and Brodrick, B. V. (1985) "Polymer grid reinforcement of asphalt". Proceedings of Association of Asphalt Paving Technologists, pp. 54, 18-44.

Brown, S. F., Thom, N. H., and Sanders, P. J. (2001) "A study of grid reinforced asphalt to combat reflection cracking". Journal of Association of Asphalt Paving Technologists, 70, pp. 543–569.

Caltabiano, M. A., and Brunton, J. M. (1991) "Reflection cracking in asphalt overlays". Journal of Association of Asphalt Paving Technologists, 60, pp. 310–330.

Chen, Q., Abu-Farsakh, M. and Tao, M. (2009) "Laboratory Evaluation of Geogrid Base Reinforcement and Corresponding Instrumentation Program". Geotechnical Testing Journal, Vol. 32, No. 6, pp. 1-10.

Elseifi, M. A., and Al-Qadi, I. L. (2003) "A simplified overlay design model against reflective cracking utilizing service life prediction", In: 82nd Transport Research Board annual meeting, Washington, D.C.

Ferrotti, G., Canestrari, F., Pasquini, E., and Virgili, A. (2012) "Experimental evaluation of the influence of surface coating on fiberglass geogrid performance in asphalt pavements". Geotextiles and Geomembranes, Vol. 34, pp. 11-18.

Guo, Z, and Zhang, Q. (1993) "Prevention of cracking progress of asphalt overlayer with glass fabric". Reflective cracking in pavements: state of the art and design recommendations. Proceedings of the Second International RILEM Conference, Liege, Belgium, 10–12, pp. 398–405.

Gurung, N. (2003) "A laboratory study on the tensile response of unbound granular base road pavement model using geosynthetics". Geotextiles and Geomembranes, Vol. 21, pp. 59-68.

Khodaii, A., Fallah, S., and Moghadas Nejad, F. (2009) "Effects of geosynthetics on reduction of reflection cracking in asphalt overlays". Geotextiles and Geomembranes, 7, pp. 137-140.

Komatsu, T., Kikuta, H., Tuji, Y., and Muramatsu, E. (1998) "Durability assessment of geogrid-reinforced asphalt concrete". Geotextile and Geomembranes, 16, pp. 257–271.

Kumar, V. V., Saride, S. and Peddinti, P. R. T. (2017) "Interfacial Shear Properties of Geosynthetic Interlayered Asphalt Overlays". Proceedings of the Geotechnical Frontiers, Orlando, USA, Geotechnical Special Publication No. 277, pp. 442-451.

Kumar, V. V., and Saride, S. (2017) "Use of Digital Image Correlation for the Evaluation of Flexural Fatigue Behavior of Asphalt Beams with Geosynthetic Interlayers". Transportation Research Record: Journal of Transportation Research Board No. 2631, pp. 55-64.

Mahrez, A., Karim, M. R., and Katman, H. Y. (2005) "Fatigue and Deformation properties of Using Glass Fiber Reinforced Bituminous Mixes". J. East Asia Society of Transportation Studies, 6, pp. 997-1007.

Miro, R., Martinez, A. H., Perez-Jimenez, F., and Botella, R. (2014) "Analysis of cracking resistance of bituminous mixtures using Fenix test". Construction and Building Materials, 59, pp. 32-38.

Murdock, J. W., and Kesler, C. E. (1958) "Effect of range of stress on fatigue strength of plain concrete beams". American Concrete Institute Journal, 55(2), pp. 221-232.

Pasquini, E., Bocci, M., Ferrotti, G., and Canestrari, F. (2012) "Laboratory characterization and field validation of geogrid-reinforced asphalt pavements". Road Materials and Pavement Design, 14, pp. 17-35.

Paul, D. K., Theivakularatnam, M., and Gnanendran, C. T. (2015) "Damage study of a lightly stabilized granular material using flexural testing". Indian Geotechnical Journal, 45(4), pp. 441-448.

Perez-Jimenez, F., Valdes, G. A., Botella, R., Miro, R., and Martinez, A. (2012) "Approach to fatigue performance using Fenix test for asphalt mixtures". Construction and Building Materials, 26, pp. 372-380.

Saride, S., and Kumar, V. V. (2017) "Influence of geosynthetic-interlayers on the performance of asphalt overlays on pre-cracked pavements". 45(3), pp. 184-196.

Shukla, S. K., and Yin, J. H. (2004) "Functions and installation of paving geosynthetics", In: 3rd Asian regional conference on geosynthetics.

Virgili, A., Canestrari, F., Grilli, A., and Santagata, F. A. (2009) "Repeated load test on bituminous systems reinforced with geosynthetics". Geotextiles and Geomembranes, 27, pp. 187-195.